J|A|C|S
ARTICLES
Published on Web 05/19/2006

Defect-Free Nanoporous Thin Films from ABC Triblock Copolymers

Joona Bang,[†,‡] Seung Hyun Kim,[§] Eric Drockenmuller,[||] Matthew J. Misner,[§] Thomas P. Russell,*[,§] and Craig J. Hawker*[,‡]

Department of Chemical and Biological Engineering, Korea University, Seoul 136-713, Republic of Korea, Materials Research Laboratory and Department of Chemistry and Biochemistry, University of California, Santa Barbara, California 93106, Department of Polymer Science and Engineering, University of Massachusetts, Amherst, Massachusetts 01003, and Laboratoire des Matériaux Polymères et Biomatériaux - UMR CNRS 5627, Université Claude Bernard Lyon, 15, Bd Latarjet, F− 69 622 VILLEURBANNE, France

Received February 2, 2006; E-mail: russell@mail.pse.umass.edu; hawker@mrl.ucsb.edu

Abstract: The self-assembly of triblock copolymers of poly(ethylene oxide-*b*-methyl methacrylate-*b*-styrene) (PEO-*b*-PMMA-*b*-PS), where PS is the major component and PMMA and PEO are minor components, provides a robust route to highly ordered, nanoporous arrays with cylindrical pores of 10−15 nm that show promise in block copolymer lithography. These ABC triblock copolymers were synthesized by controlled living radical polymerization, and after solvent annealing, thin films showing defect-free cylindrical microdomains were obtained. The key to the successful generation of highly regular, porous thin films is the use of PMMA as a photodegradable mid-block which leads to nanoporous structures with an unprecedented degree of lateral order. The power of using a triblock copolymer when compared to a traditional diblock copolymer is evidenced by the ability to exploit and combine the advantages of two separate diblock copolymer systems, the high degree of lateral ordering inherent in PS-*b*-PEO diblocks plus the facile degradability of PS-*b*-PMMA diblock copolymer systems, while negating the corresponding disadvantages, poor degradability in PS-*b*-PEO systems and no long-range order for PS-*b*-PMMA diblocks.

Introduction

The self-assembly of block copolymers has attracted considerable attention as a simple, versatile route to nanostructured materials[1] and has led to the development of block copolymer lithography as a viable technique for the fabrication of microelectronic devices.[2−15] As a "bottom up" molecular system, block copolymer lithography allows exquisite control over the size and, to a lesser extent, the two-dimensional arrangement of nanoscale features. By simply changing the molecular weight and/or the relative ratio of constituent blocks, the morphology and size scales of the features can be controlled. In terms of thin films, the nanoporous materials derived from block copolymers have also been actively studied as nano-templates, membranes, separation media, high surface area support for catalysis, and sensors.[1,8,12,14,16−28]

Several routes to generate nanoporous films via block copolymer self-assembly have been reported since Nakahama and co-workers first demonstrated the formation of nanoporous polymer films from a siloxane-functionalized poly(styrene-*b*-isoprene) system.[29] The most common strategy is to remove

[†] Korea University.
[‡] University of California.
[§] University of Massachusetts.
[||] Université Claude Bernard Lyon.

(1) Hawker, C. J.; Wooley, K. L. *Science* **2005**, *309*, 1200.
(2) Park, M.; Harrison, C.; Chaikin, P. M.; Register, R. A.; Adamson, D. H. *Science* **1997**, *276*, 1401−1404; Hawker, C. J.; Russell, T. P. *MRS Bull.* **2005**, *30*, 952−967; Segalman, R. A. *Mater. Sci. Eng., R* **2005**, *48*, 191−226.
(3) Templin, M.; Franck, A.; Du Chesne, A.; Leist, H.; Zhang, Y.; Ulrich, R.; Schadler, V.; Wiesner, U. *Science* **1997**, *278*, 1795−1798.
(4) Spatz, J. P.; Herzog, T.; Moessmer, S.; Ziemann, P.; Moeller, M. *Adv. Mater.* **1999**, *11*, 149−153.
(5) Lopes, W. A.; Jaeger, H. M. *Nature* **2001**, *414*, 735−738.
(6) Cheng, J. Y.; Ross, C. A.; Chan, V. Z. H.; Thomas, E. L.; Lammertink, R. G. H.; Vancso, G. J. *Adv. Mater.* **2001**, *13*, 1174−1178.
(7) Cheng, J. Y.; Ross, C. A.; Thomas, E. L.; Smith, H. I.; Vancso, G. J. *Appl. Phys. Lett.* **2002**, *81*, 3657−3659.
(8) Drockenmuller, E.; Li, L. Y. T.; Ryu, D. Y.; Harth, E.; Russell, T. P.; Kim, H. C.; Hawker, C. J. *J. Polym. Sci., Part A: Polym. Chem.* **2005**, *43*, 1028−1037.
(9) Kim, H.-C.; Jia, X.; Stafford, C. M.; Kim, D. H.; McCarthy, T. J.; Tuominen, M.; Hawker, C. J.; Russell, T. P. *Adv. Mater.* **2001**, *13*, 795−797.
(10) Black, C. T.; Guarini, K. W. *J. Polym. Sci., Part A: Polym. Chem.* **2004**, *42*, 1970−1975.
(11) Bal, M.; Ursache, A.; Tuominen, M. T.; Goldbach, J. T.; Russell, T. P. *Appl. Phys. Lett.* **2002**, *81*, 3479−3481.
(12) La, Y. H.; Edwards, E. W.; Park, S. M.; Nealey, P. F. *Nano Lett.* **2005**, *5*, 1379−1384.
(13) Kim, D. H.; Kim, S. H.; Lavery, K.; Russell, T. P. *Nano Lett.* **2004**, *4*, 1841−1844.
(14) Zhang, Q.; Xu, T.; Butterfield, D.; Misner, M. J.; Ryu, D. Y.; Emrick, T.; Russell, T. P. *Nano Lett.* **2005**, *5*, 357−361.
(15) Stoykovich, M. P.; Muller, M.; Kim, S. O.; Solak, H. H.; Edwards, E. W.; de Pablo, J. J.; Nealey, P. F. *Science* **2005**, *308*, 1442−1446.
(16) Liu, G.; Ding, J.; Hashimoto, T.; Kimishima, K.; Winnik, F. M.; Nigam, S. *Chem. Mater.* **1999**, *11*, 2233−2240.
(17) Liu, G.; Ding, J.; Stewart, S. *Angew. Chem., Int. Ed.* **1999**, *38*, 835−838.
(18) Segalman, R. A.; Hexemer, A.; Kramer, E. J. *Macromolecules* **2003**, *36*, 6831−6839.
(19) Segalman, R. A.; Yokoyama, H.; Kramer, E. J. *Adv. Mater.* **2001**, *13*, 1152−1156.
(20) Johnson, B. J. S.; Wolf, J. H.; Zalusky, A. S.; Hillmyer, M. A. *Chem. Mater.* **2004**, *16*, 2909−2917.
(21) Olayo-Valles, R.; Lund, M. S.; Leighton, C.; Hillmyer, M. A. *J. Mater. Chem.* **2004**, *14*, 2729−2731.

10.1021/ja0608141 CCC: $33.50

the minor component selectively after self-assembly and, as a result, generate nanoscopic pores in a matrix of the majority component. A wide variety of diblock copolymers have been used, in some cases incorporating functionality to cross-link the majority component or homopolymers to modify the morphology. In contrast, only a small number of ABC-triblock copolymers[27,28] have been studied, which is surprising given their richer phase morphologies. One of the major shortcomings with all of these systems is the presence of defects or grain boundaries in the nanoporous array, which limits the range of applications for these nanoscale templates to those that do not require registration or alignment.

To overcome the drawback of lateral order and defects, we have recently demonstrated that the self-assembly of polystyrene-*b*-poly(ethylene oxide) (PS-*b*-PEO) diblock copolymers leads to a highly ordered arrays of cylindrical microdomains of PEO in a PS matrix. By the use of solvent evaporation and annealing, defect-free arrays can be achieved over large lateral areas (ca. 10 μm $\times$ 10 μm).[30,31] In comparison to the classical poly(styrene-*b*-methyl methacrylate) (PS-*b*-PMMA) diblock copolymer system, the long-range order in PS-*b*-PEO arises from the stronger nonfavorable interactions between PS and PEO, combined with the directionality of solvent evaporation. Although a high degree of long-range lateral order of PEO cylindrical microdomains is obtained with few defects, it is extremely difficult to selectively remove the PEO block by simple etching processes. Hillmyer and co-workers recently reported[28] the successful use of iodic acid to achieve this. However, the degradation requires immersion in a 57 wt % aqueous HI solution at 60 °C for 5 days and was only applicable to bulk samples and not thin films. This is in direct contrast to the classical PS-*b*-PMMA system discussed above where irradiation with UV light for less than 10 min leads to degradation of the PMMA and generation of porosity.

In this manuscript, a strategy that combines the facile degradation of PS-*b*-PMMA with the long-range lateral order of PS-*b*-PEO-based systems to give defect-free, porous thin films suitable for block copolymer lithography is presented. By employing a triblock copolymer system, it is envisaged that the advantages of different diblock copolymer systems can be combined while at the same time negating the corresponding disadvantages such as poor degradability in PS-*b*-PEO diblocks and a lack of long-range order for PS-*b*-PMMA systems. To achieve these desired characteristics, the required triblock copolymers have a general PS-*b*-PMMA-*b*-PEO structure in which the central PMMA block imparts degradability to the system while the terminal PEO block permits long-range ordering. The use of triblock copolymers provides a simple route to the generation of well-ordered nanoscopic templates that can be potentially used for applications requiring the precise control of location and orientation of nanoscopic domains, such as high-density, addressable storage media or for registration with an underlying pattern.

Results and Discussion

The synthesis of a library of ABC triblock copolymers, poly(ethylene oxide-*b*-methyl methacrylate-*b*-styrene) (PEO-*b*-PMMA-*b*-PS), with various PMMA block lengths necessitated the use of a living free radical polymerization process. Due to its synthetic versatility and ability to polymerize methyl methacrylate (MMA) under controlled conditions, reversible addition fragmentation chain transfer (RAFT) polymerization[32] was the living free radical polymerization procedure of choice. The sequence of polymerization was therefore ethylene oxide, followed by MMA and styrene with the volume fraction of PEO and PMMA blocks being controlled to allow the formation of cylindrical PEO/PMMA microdomains.

In designing the RAFT macroinitiator based on PEO, one of the major hurdles is the limited range of RAFT agents that act as efficient initiators for the controlled polymerization of methyl methacrylate. The tedious and low-yielding synthesis of tertiary, dithioester RAFT agents derived from AIBN derivatives was circumvented by the recent development by a variety of groups[33] of stabilized secondary, dithioester RAFT agents. These dithioester derivatives are based on the realization that a tertiary radical is not required for efficient initiation of MMA if two radical stabilizing groups are present. As a result, synthetic accessibility of these MMA-capable RAFT agents is greatly enhanced and a variety of efficient functionalization strategies are now available. To facilitate the synthesis of RAFT macroinitiators, well-defined monomethoxy-terminated PEO derivatives were used as starting materials, and the desired PEO−RAFT macroinitiator was prepared by end-group modification via a two-step procedure involving the initial esterification of monomethoxy PEO with α-bromophenylacetic acid to give the phenyl acetate derivative, **1**. Coupling of **1** with the anion derived from the reaction of phenylmagnesium bromide with carbon disulfide gives the dithioester, **2**. The RAFT agent at the chain end of **2** is stabilized by both the phenyl ring as well as the ester group and is capable of controlling the polymerization of MMA (Scheme 1). The incorporation and quantification of the RAFT group at the termini of the PEO chains was confirmed by a variety of techniques. Size-exclusion chromatography in combination with a photodiode array detector confirmed the presence of the dithioester group through the characteristic UV absorbance of the dithioester group at ca. 320 nm. Quantification of chain-end functionalization could be accomplished by ^{1}H NMR and integration of the unique signals for the CH−S group at 5.73 ppm and the aromatic protons ortho to the C=S group at 8.02 ppm followed by comparison with the resonances for the PEO chain (Figure 1a).

Reaction of **2** with MMA and AIBN at 70 °C gave the diblock copolymer, **3**, which was then used to initiate the polymerization

(22) Mao, H.; Arrechea, P. L.; Bailey, T. S.; Johnson, B. J. S.; Hillmyer, M. A. *Faraday Discuss.* **2005**, *128*, 149−162.
(23) Li, M.; Douki, K.; Goto, K.; Li, X.; Coenjarts, C.; Smilgies, D. M.; Ober, C. K. *Chem. Mater.* **2004**, *16*, 3800−3808.
(24) Liang, C.; Hong, K.; Guiochon, G. A.; Mays, J. W.; Dai, S. *Angew. Chem., Int. Ed.* **2004**, *43*, 5785−5789.
(25) Pai, R. A.; Humayun, R.; Schulberg, M. T.; Sengupta, A.; Sun, J.-N.; Watkins, J. J. *Science* **2004**, *303*, 507−511.
(26) Xu, Y.; Gu, W.; Gin, D. L. *J. Am. Chem. Soc.* **2004**, *126*, 1616−1617.
(27) Sugihara, S.; Kanaoka, S.; Aoshima, S., *J. Polym. Sci., Part A: Polym. Chem.* **2004**, *42*, 2601−2611.
(28) Rzayev, J.; Hillmyer, M. A. *Macromolecules* **2005**, *38*, 3−5; Rzayev, J.; Hillmyer, M. A. *J. Am. Chem. Soc.* **2005**, *127*, 13373−13379; Mao, H.; Hillmyer, M. A. *Soft Matter* **2006**, *2*, 57.
(29) Lee, J. S.; Hirao, A.; Nakahama, S. *Macromolecules* **1988**, *21*, 274−276.
(30) Kim, S. H.; Misner, M. J.; Xu, T.; Kimura, M.; Russell, T. P. *Adv. Mater.* **2004**, *16*, 226−231.
(31) Kim, S. H.; Misner, M. J.; Russell, T. P. *Adv. Mater.* **2004**, *16*, 2119−2123.
(32) Monteiro, M. J. *J. Polym. Sci., Part A: Polym. Chem.* **2005**, *43*, 5643−5651; Perrier, S.; Takolpuckdee, P. *J. Polym. Sci., Part A: Polym. Chem.* **2005**, *43*, 5347−5393.
(33) Li, C.; Benicewicz, B. C. *J. Polym. Sci., Part A: Polym. Chem.* **2005**, *43*, 1535−1543; Takolpuckdee, P.; Mars, C. A.; Perrier, S.; Archibald, S. J. *Macromolecules* **2005**, *38*, 1057−1060.

Scheme 1. Synthesis of PEO-*b*-PMMA-*b*-PS Triblock Copolymers, **4**, by RAFT Polymerization

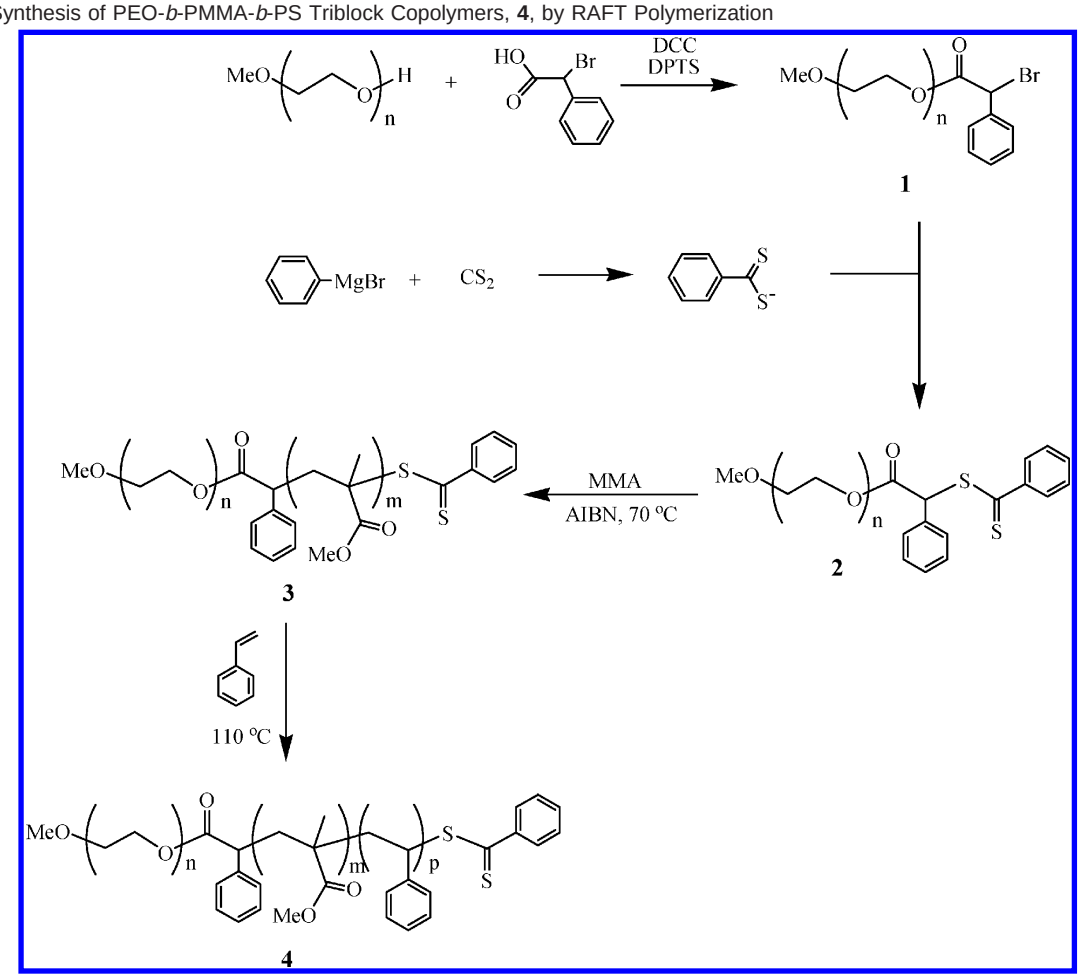

of styrene to give the desired triblock copolymer, **4**. The fidelity of the growth process could be confirmed by SEC, which shows the controlled increase in molecular weight on chain extension from the PEO−RAFT macroinitiator, **2**, to the PEO−PMMA diblock, **3**, and finally to the PEO-*b*-PMMA-*b*-PS triblock copolymers, **4** (Figure 2). The relative amount of each block and their associated molecular weights could be determined by ^{1}H NMR based on the known molecular weight of 5000 amu for the starting PEO block ($n = 112$) (Figure 1b).

The fidelity of the RAFT polymerization process allowed full characterization of all the triblock copolymers synthesized, and the stability of the intermediate macroinitiator and subsequent diblock copolymers permitted the molecular weight of the PMMA and PS blocks to be accurately controlled. As a result, a library of triblock copolymers were prepared in which the overall bulk morphologies were maintained as a bulk polystyrene domain with cylindrical microdomains of PMMA/PEO (Table 1).

Interestingly, the richer phase behavior of ABC triblock copolymers permitted a range of nanostructures to be studied within this overall cylindrical domain space. This allows the effect of morphology and phase separation of the PMMA and PEO blocks on the thin-film behavior and degradability to be examined by varying the molecular weight of the middle PMMA block from 1500 to 16 000 amu. The overall molecular weights of **4** were therefore 20 000−121 000 g/mol, and in all cases, narrow polydispersity indexes (PDI < 1.1) were obtained with no detectable amounts of homopolymer or diblock copolymer contaminants.

Initial morphological studies of the ABC triblock copolymers involved SAXS experiments on bulk samples, and representative examples are shown in Figure 3. The three PEO-*b*-PMMA-*b*-PS triblock copolymers, having volume fraction of PS between 74 and 84% (**4b**, **4e**, and **4h**), exhibited a cylindrical microdomain morphology as evidenced by higher order reflections at q values of $1{:}\sqrt{3}{:}\sqrt{4}{:}\sqrt{7}{:}\sqrt{9}$ relative to the first-order reflection. The other triblocks, such as **4a** which had the lowest weight fraction of PS, exhibited only a first-order peak. The absence of higher-order reflections is presumably due to the lack of the long-range order in these bulk samples.

To investigate the morphology of the corresponding thin films, scanning force microscopy, SFM, was used, and Figure 4 shows the SFM phase images of a selection of three triblock copolymers on silicon substrates, **4a**, **4b**, and **4e**, shortly after spin-coating. The resulting structures are poorly defined, and it is difficult to identify any morphology or orientation of the microdomains. However, if the films are annealed in the presence of benzene vapor and a controlled humidity atmosphere (70−90% relative humidity), well-defined structures are observed, where arrays of nanoscopic, cylindrical microdomains of the minor components are seen at the surface of films for all three triblocks (Figure 5a−c). As these systems are intended as templates for block copolymer lithography, it was important to examine the nanostructure present at the substrate surface as

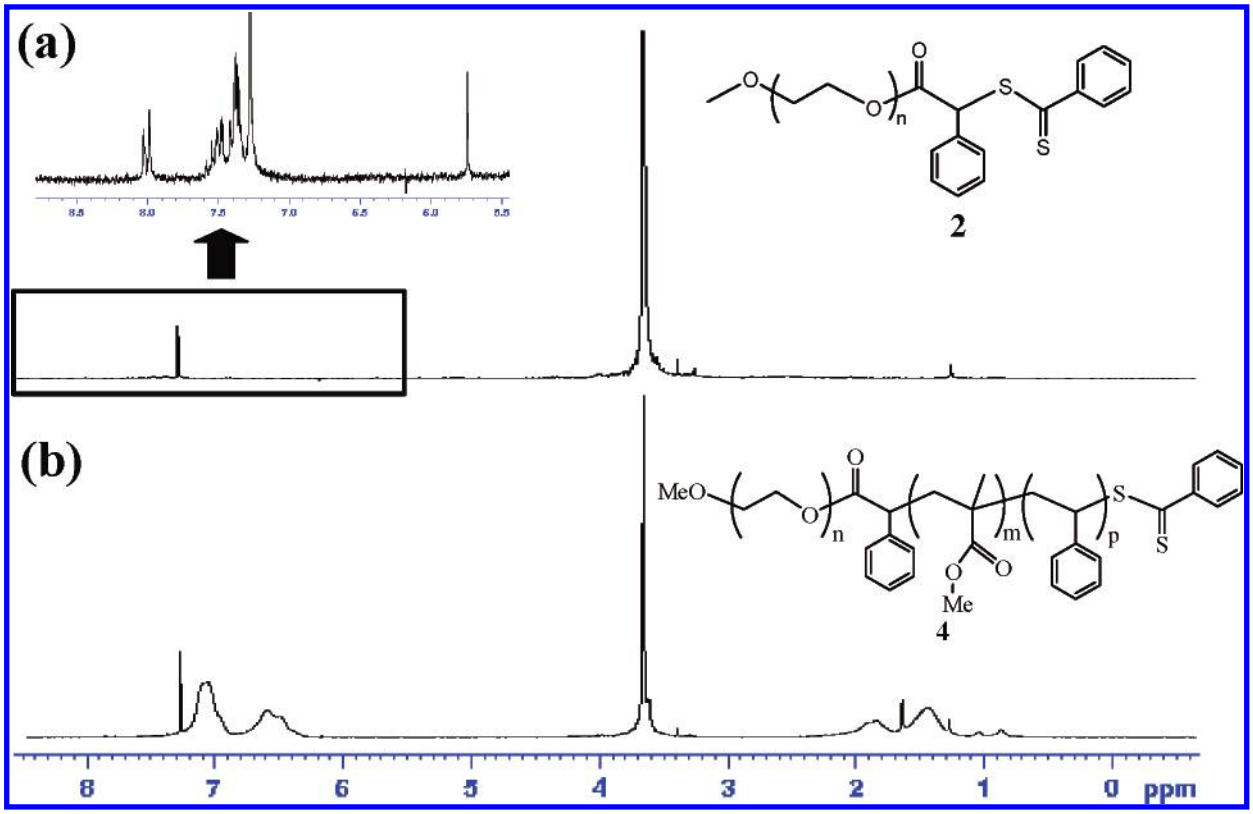

Figure 1. ^{1}H NMR spectrum of (a) PEO−RAFT macroinitiator, **2**, and (b) PS-*b*-PMMA-*b*-PEO triblock copolymer, **4**. (Inset to a) Magnification of the end group of PEO−RAFT macroinitiator.

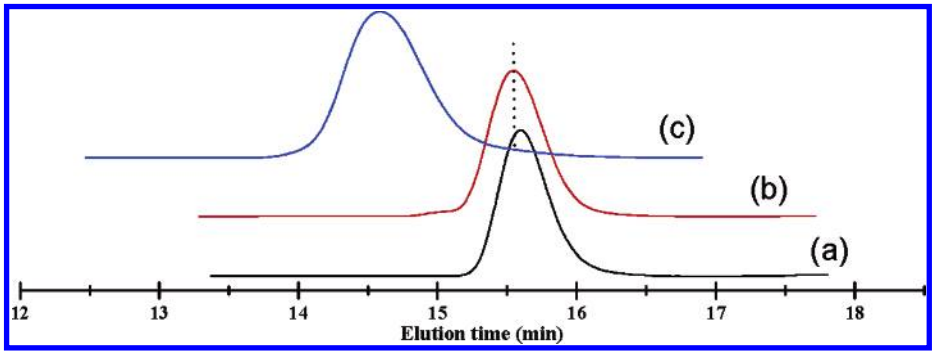

Figure 2. SEC traces for (a) PEO−RAFT, **2** (M_n = 5400 amu; PDI = 1.04); (b) PS-*b*-PEO diblock, **3** (M_n = 6900 amu; PDI = 1.06); and (c) PS-*b*-PMMA-*b*-PEO triblock copolymer, **4a** (M_n = 20 800 amu; PDI = 1.05).

Table 1. Sample Characteristics of PS-*b*-PMMA-*b*-PEO Triblock Copolymer

sample	M_{PS} (kDa)	M_{PMMA} (kDa)	M_{PEO} (kDa)	f_{PS}	f_{PMMA}	f_{PEO}	M_w/M_n	D_{c-c} (nm)[a]
4a	13.5	1.5	5.0	0.69	0.07	0.24	1.03	22.9
4b	19.4	2.6	5.0	0.74	0.08	0.18	1.03	27.6
4c	22.6	3.0	5.0	0.76	0.09	0.16	1.05	28.1
4d	35.5	5.0	5.0	0.80	0.10	0.10	1.06	33.3
4e	32.4	6.0	5.0	0.77	0.13	0.11	1.05	36.4
4f	45.0	6.5	5.0	0.81	0.10	0.09	1.05	37.3
4g	50.6	11.7	5.0	0.77	0.16	0.07	1.03	48.5
4h	100.0	16.0	5.0	0.84	0.12	0.04	1.07	58.7

[a] Measured by SAXS ($D_{c-c} = 4\pi/\sqrt{3}q^*$).

well, because it may be significantly different from the surface structure at the air interface.

The wafer−polymer interface was therefore examined by first removing the substrate and floating of the polymeric film using HF followed by flipping of the film and examining the "bottom" side by SFM. Significantly, the same structure was observed at this interface as compared to the surface, which indicates that the cylindrical domains span the entire thickness of films and are oriented normal to the film surface. Of perhaps greater importance is the observation that these triblock copolymers films develop a defect-free, hexagonally packed cylindrical array as was observed for the PS-*b*-PEO diblock copolymers.[34] It is noteworthy that the incorporation of the middle block has little effect on the ordering behavior of PS and PEO, which suggests that a wide range of structural and functional units may be incorporated as a middle block without disrupting long-range ordering, further enhancing the potential applications of these systems.

(34) As with the case of PEO-*b*-PS diblock copolymers, it should be also noted that a certain level of the relative humidity also plays an important role on the long-ranged ordering. For example, the solvent annealing below the relative humidity of 70% does not induce the long-ranged ordering. In this case, all cylinders were oriented horizontally to the substrate (data not shown). An optimal relative humidity on the long-ranged ordering is between 70 and 90% for these PEO-*b*-PMMA-*b*-PS triblock copolymers.

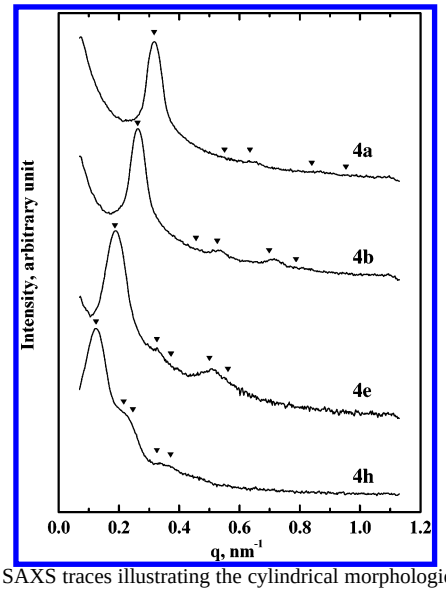

Figure 3. SAXS traces illustrating the cylindrical morphologies for PEO-*b*-PMMA-*b*-PS triblock copolymers **4a**, **4b**, **4e**, and **4h**. The arrows indicate the possible reflections at q^*/q spacings of $1:\sqrt{3}:\sqrt{4}:\sqrt{7}:\sqrt{9}$ for cylindrical morphology.

The perfection of order is dramatically shown in the triangulation map in Figure 5d−f, where every domain center is connected by a line to the adjacent domain centers. Each "perfect" domain with six nearest neighbors is colored blue, and defects with five or seven nearest neighbors are colored red and yellow, respectively. As seen in Figure 5d, every domain has six nearest neighbors, and this high degree of lateral order was found to extend over large areas for all triblock copolymers. The domain spacing calculated from the SFM images exactly matches that measured by SAXS (see Table 1). However, there is not enough phase contrast to identify all three phases in the triblock copolymer film by SFM, and it is impossible to state whether the cylindrical microdomains are composed of a single mixed PEO/PMMA phase or distinct PEO and PMMA phases.

The selective removal of the minor components, cross-linking of the major component, and generation of a nanoporous structure in PS-*b*-PMMA-*b*-PEO triblock copolymers films were achieved by deep UV irradiation followed by acetic acid rinsing. This treatment is well-known to degrade and remove PMMA but does not induce any cleavage or degradation in PS-*b*-PEO diblock copolymer films. Figure 6 shows TEM images of six triblock copolymer films after UV irradiation and acetic acid rinsing.

For **4a** and **4b**, contrary to expectations, the minor components were only partially removed and in some areas not removed at all (Figure 6a,b). The same results were observed for different film thickness and for even longer UV exposure times. When the length of the PMMA block increases (**4d**), essentially all of the microdomains were removed (Figure 6c), and for **4e** and **4g**, which have PMMA blocks of 6000 and 11 700 amu respectively, it was found that a nanoporous structure was successfully produced after UV irradiation. Significantly, this irradiation and subsequent washing did not induce any change in the film structure, and highly oriented, defect-free, nanoporous films were prepared (Figure 6c,d). It is also evident from all of the TEM images that the nanopores span the entire film. However, it is apparent from these samples that there is an optimal molecular weight for the triblock copolymer systems. For the nanoporous template obtained from **4h**, which has the longest PMMA block and the largest overall molecular weight, cylinder domains were still oriented perpendicularly to the substrate; however, the long-ranged ordering was not attained, which may be due to a reduced mobility for these higher molecular weights (Figure 6f).

From these results, it is apparent that PS-*b*-PMMA-*b*-PEO triblock copolymers can be used to generate highly ordered nanoporous templates with both a minimum and maximum length of the PMMA block for defect-free porous structures after UV irradiation. To understand the origin of this lower critical molecular weight (<5.0 kDa) in greater detail, thin-film morphologies of a range of samples before UV exposure were examined. As a representative example, Figure 7a,b shows the TEM images of **4b** (PMMA = 2.6 kDa and PEO = 5.0 kDa) and **4e** (PMMA = 6.0 kDa and PEO = 5.0 kDa) prior to UV irradiation, respectively. It is immediately apparent that the two triblock copolymers exhibit totally different phase behavior with the lower molecular weight derivative, **4b**, showing a single diffuse cylindrical phase, whereas the higher molecular weight triblock, **4e**, reveals a structured core−shell morphology (see schematic representations). Examination of the DSC traces for these triblock copolymers provides further evidence to support the morphology. As can be seen in Figure 8, for a constant molecular weight of PEO (5.0 kDa), the crystallinity of the PEO block decreases significantly as the molecular weight of the PMMA block increases from 1.5 to 2.6 kDa and is totally absent at 6.0 kDa. The miscibility of PMMA and PEO for the lower molecular weight blocks found in **4a** allows the formation of a single PMMA−PEO cylindrical domain, and the additional chain length of PMMA confers enough chain mobility for the PEO chain to crystallize. As the molecular weight of the PMMA block increases, the miscibility decreases, which results in a phase separated core−shell structure for which the confinement

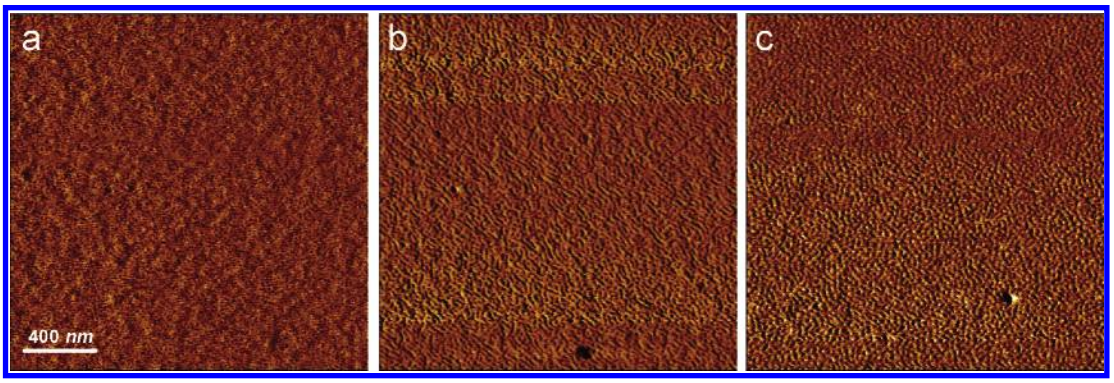

Figure 4. SFM phase images for PEO-*b*-PMMA-*b*-PS triblock copolymer thin films of (a) **4a**, (b) **4b**, and (c) **4e** after spin-coating.

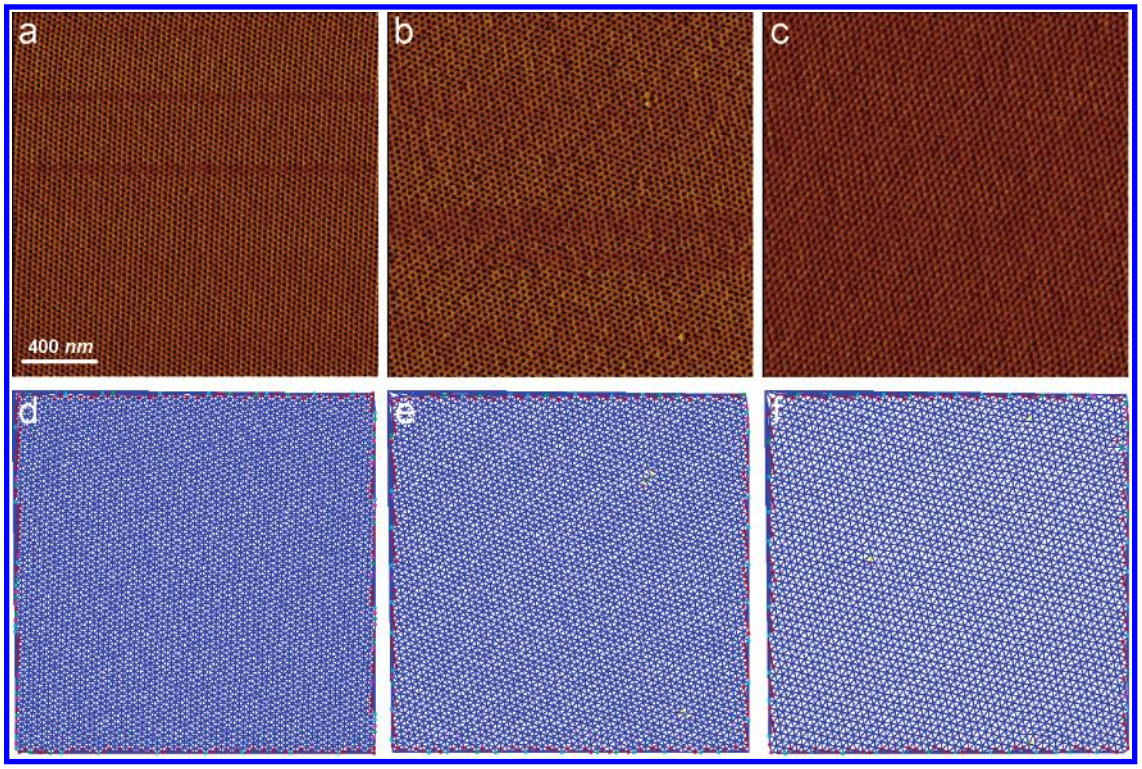

Figure 5. SFM phase images for PEO-*b*-PMMA-*b*-PS triblock copolymer thin films of (a) **4a**, (b) **4b**, and (c) **4e** after annealing for 12 h in a benzene vapor with controlled humidity. (d), (e), and (f) correspond to triangulation images of SFM images shown in (a), (b), and (c), respectively.

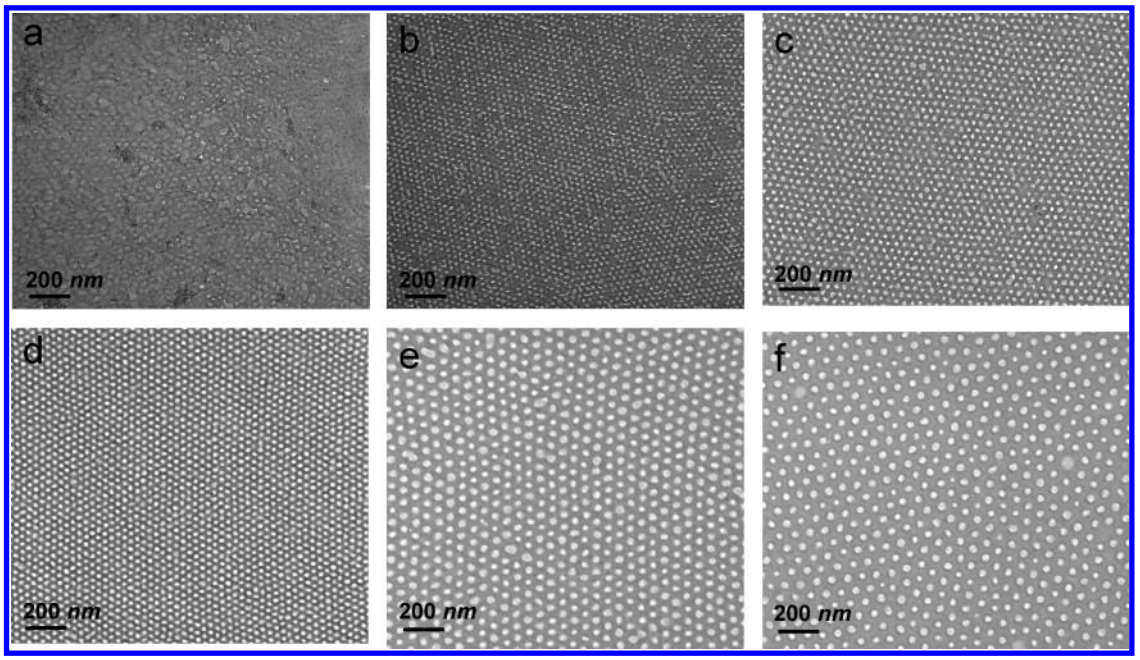

Figure 6. TEM images (top view) for PEO-*b*-PMMA-*b*-PS triblock copolymer thin films of (a) **4a**, (b) **4b**, (c) **4d**, (d) **4e**, (e) **4f**, and (f) **4h** after solvent annealing, followed by UV irradiation. The bright circles correspond to nanopores where the cylindrical microdomains are removed after UV irradiation.

of the PEO to the central domain does not allow the PEO chains to crystallize. This transition from phase-mixed to phase-separated microdomains also provides a rationale for the changes observed for photodegradation of the triblock copolymers. Previous work has shown that the photochemical degradation of PMMA is severely retarded in the presence of solvents such as tetrahydrofuran, which contain an ether linkage, as well as in polymer blends with poly(vinyl acetate).[35] It is therefore proposed that a similar effect is operating in these triblock copolymer systems where the photodegradation of PMMA is retarded at lower molecular weights of PMMA due to the formation of a miscible blend with PEO and only when complete phase separation occurs does the central PMMA block undergo efficient photodegradation.

These results further highlight the importance of structural control in polymer materials where small changes in the chain length of the PMMA block leads to dramatically different

(35) Kaminska, A.; Swiatek, M. *J. Therm. Anal.* **1996**, *46*, 13830−1390.

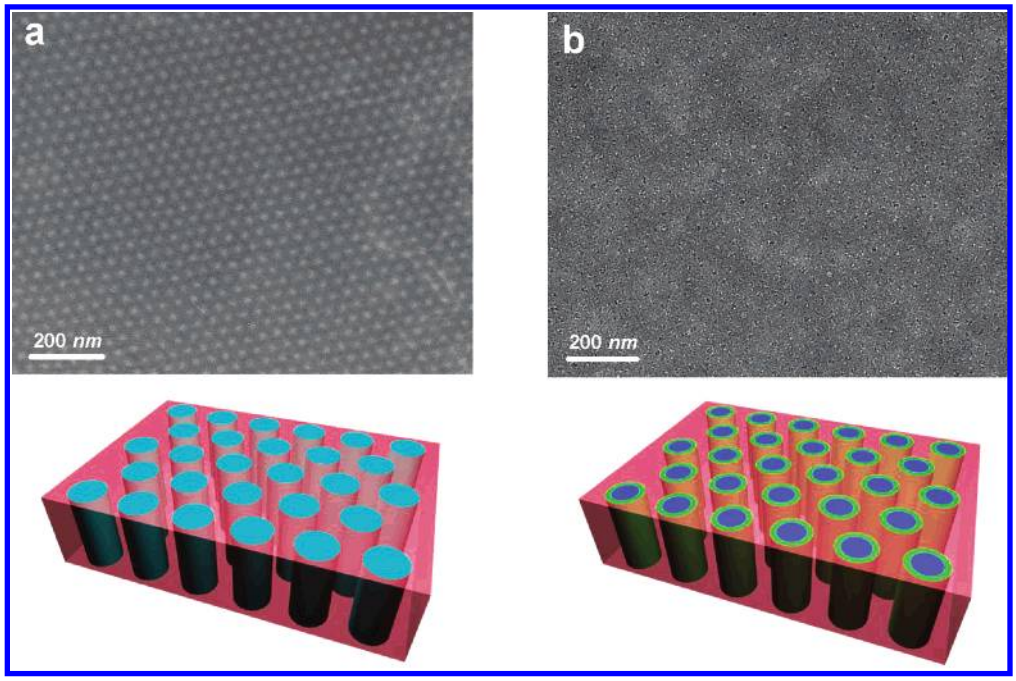

Figure 7. TEM images (top view) for PEO-*b*-PMMA-*b*-PS triblock copolymer thin films of (a) **4b** and (b) **4e** after solvent annealing. The schematics below illustrate the possible structures of the cylindrical microdomains.

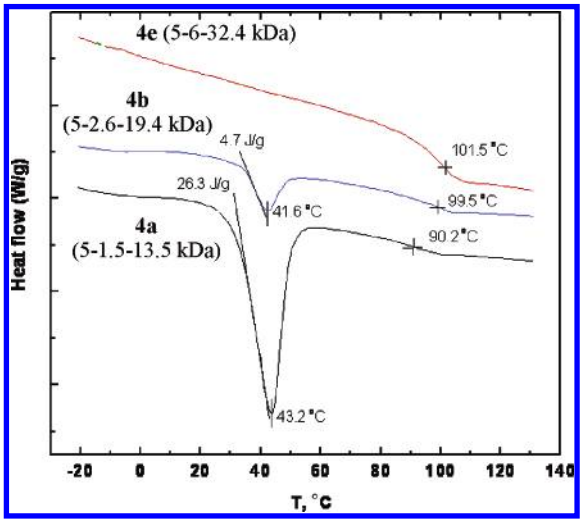

Figure 8. DSC traces for PEO-*b*-PMMA-*b*-PS triblock copolymer thin films of (a) **4a**, (b) **4b**, and (c) **4e**.

performance in block copolymer lithography. Only when the PMMA block forms a separate phase in a cylindrical core−shell morphology can UV irradiation effectively degrade the PMMA block leading to generation of the block copolymer template.

Conclusion

Exploiting the facile degradability of PS-*b*-PMMA block copolymers, combined with the long-range ordering of PS-*b*-PEO systems, has allowed the development of a versatile methodology for the fabrication of highly ordered arrays of nanopores via the self-assembly of triblock copolymers. The synthesis of PS-*b*-PMMA-*b*-PEO triblock copolymers by RAFT polymerization allows the middle PMMA block to function as a sacrificial block while the terminal PEO block directs phase separation. This allows templates for block copolymer lithography to be prepared by initial solvent annealing followed by UV irradiation to degrade the PMMA block and generate an almost perfect hexagonal array of 10−15 nm diameter cylindrical holes. Significantly, this behavior was found to depend critically on the molecular weight and phase behavior of the central PMMA block, and only when the PMMA block formed a distinct microdomain did facile degradation occur. When the PMMA is miscible with PEO, phase separation occurs to give well-ordered arrays of PMMA/PEO cylinders in a PS matrix; however, photochemical degradation of the PMMA chains is retarded, and no template is formed. The ability to tune the complex phase morphologies of triblock copolymer systems by synthetically varying the block lengths and chemical nature of each block is a powerful tool for the fabrication of functional nanostructures. By combining the desired features of multiple block copolymers into a single system, greater variability and nanostructural control is obtained when compared to traditional diblock copolymer systems.

Experimental Section

Materials were characterized by ^{1}H nuclear magnetic resonance (NMR), using a Bruker 200 MHz spectrometer with the residual solvent signal as an internal reference. Gel permeation chromatography was performed in THF on a Waters chromatograph equipped with four 5-μm Waters columns (300 × 7.7 mm) connected in series with increasing pore size (100, 1000, 10 000, and 1 000 000 Å). Waters 410 differential refractometer index (DRI) and 996 photodiode array detectors were employed. The molecular weights of the polymers were calculated relative to linear PMMA and PS standards. The modulated differential scanning calorimetry (DSC) measurements were performed with a TA Instruments, DSC 2920, and with a ramp rate of 4° min^{-1}. Glass-transition temperatures (T_g) were taken as the midpoint of the inflection tangent, upon the third heating scan. Infrared spectra (IR) were obtained on Perkin−Elmer Spectrum BX FT-IR system using either diffuse reflectance sampling accessories or drop deposition onto NaCl plates.

4-(Dimethylamino)pyridinium-4-toluenesulfonate (DPTS) was prepared through the reaction of 4-(dimethylamino)pyridine (DMAP) and anhydrous *p*-toluenesulfonic acid (PTSA) in benzene according to the

literature.[36] PEO was dried by dissolving in toluene, followed by azeotropic distillation at 60 °C; styrene was stored over CaH_2 and then vacuum distilled, and 2,2′-azobisisobutyronitrile (AIBN) was recrystallized from methanol. All other reagents were purchased from commercial sources and used as received unless otherwise noted.

α-Bromo-phenylacetate Terminated Poly(ethylene oxide), 1. Monomethoxy poly(ethylene oxide) (M_n = 5 000, PDI = 1.05) (10.0 g, 2.00 mmol) and DMAP (49 mg, 0.4 mmol) were dissolved in toluene (20 mL) and dried by azeotropic distillation. To this solution was added dichloromethane (30 mL), α-bromophenylacetic acid (1.29 g, 6.00 mmol), DPTS (295.0 mg, 1 mmol), and dicyclohexylcarbodiimide (DCC) (2.07 g, 10 mmol). The reaction mixture was then stirred at room temperature for 12 h, filtered, and added dropwise to hexane (500 mL). The crude product was filtered, and the desired functionalized PEO derivative, **1**, was further purified by precipitation into hexane. Yield: 67%. M_n: 5 400. PDI: 1.04. ^{1}H NMR (200 MHz, $CDCl_3$) δ: 3.24−4.05 (s, OCH_2), 5.40 (s, CH), and 7.32−7.61 (m, ArH).

α-(Dithiobenzoate)-phenylacetate Terminated PEO, RAFT−PEO Macroinitiator, 2. Carbon disulfide (165 mg, 0.13 mL, 2.2 mmol) was added dropwise to a solution of phenylmagnesium bromide (0.73 mL of a 3.0 M solution in diethyl ether, 2.2 mmol) in dry tetrahydrofuran (30 mL) at 50 °C. The reaction mixture was stirred for 30 min under nitrogen, resulting in a dark-red solution. To this solution was added the functionalized PEO, **1** (5.5 g, 1.1 mmol) dissolved in dry tetrahydrofuran (10 mL), and the reaction mixture was heated at reflux for 24 h. The solution was then filtered and precipitated into hexane (500 mL) to yield the PEO−RAFT macroinitiator, **2**, as a pink solid. Yield: 84%. M_n: 5,400. PDI: 1.04. ^{1}H NMR (200 MHz, $CDCl_3$) δ: 3.25−4.06 (s, OCH_2), 5.74 (s, CH), 7.31−7.60 (m, ArH), and 7.95 − 8.05 (d, ArCSS).

PEO-*b*-PMMA−RAFT Diblock Copolymer, 3. A mixture of the PEO−RAFT macroinitiator, **2** (1.0 g, 0.2 mmol), MMA (2.0 g, 20 mmol), and AIBN (5 mg, 0.03 mmol) was dissolved in benzene (1 mL) and degassed by performing the three freeze−pump−thaw cycles. The glass ampule was sealed under vacuum and then heated to 70 °C for 5 h (conversion of MMA was ca. 50%). After this time, the viscous reaction mixture was dissolved in dichloromethane (5 mL) and precipitated into hexane (400 mL) to give the diblock copolymer, **3**, as a pink solid. Yield: 43%. ^{1}H NMR (200 MHz, $CDCl_3$) δ: 0.65−2.08 (m, CH_2, CH, CH_3), 3.45−3.60 (s, OCH_3), and 3.64−3.80 (s, OCH_2); M_n = 10 200; PDI = 1.05.

PEO-*b*-PMMA-*b*-PS Triblock Copolymers, 4. The RAFT-terminated diblock copolymer, **3** (0.5 g, 0.05 mmol) and styrene (3.0 g, 29 mmol), was dissolved in benzene (1 mL), and the reaction mixture was degassed by three freeze−pump−thaw cycles. The glass ampule was sealed under vacuum and then heated at 115 °C for 20 h (conversion of styrene was ca. 70%). The reaction mixture was dissolved in dichloromethane (5 mL) and precipitated into hexane (250 mL). To remove any unfunctionalized PEO homopolymers, the precipitate was further dissolved in dichloromethane (5 mL) and reprecipitated in methanol (250 mL) to yield purified the triblock copolymer, **4**, as a pink solid. Yield: 65%; ^{1}H NMR (200 MHz, $CDCl_3$) δ: 0.74−2.30 (m, CH_2, CH, CH_3), 3.45−3.64 (s, OCH_3), 3.64−3.78 (s, OCH_2), and 6.28−7.34 (m, ArH); M_n = 45 500; PDI = 1.06.

Preparation of the Thin Films. General Procedures. The PEO-*b*-PMMA-*b*-PS triblock copolymers were spin coated from benzene solutions onto silicon substrates and then annealed in a benzene atmosphere, where the relative humidity was controlled between 70 and 90%. The film thickness was controlled by adjusting the solution concentration and the spinning speed.[30] To cleave the PMMA block, the copolymer films were irradiated by deep UV light with a wavelength of 254 nm at a dose of 25 J cm^{-2} (XX-15S; UVP Inc.) under vacuum for 10 min, rinsed in acetic acid, and then rinsed in water.

Characterization. To determine the bulk morphologies for triblock copolymers, small-angle X-ray scattering (SAXS) was performed using a rotating anode with CuK_α X-rays (λ = 1.54 Å). A sample-to-detector distance of 1.7 m was used to access the necessary q range. The two-dimensional (2-D) SAXS images were azimuthally averaged to produce one-dimensional profiles of intensity, I, vs wavevector, q, using the 2-D data reduction program FIT2D.

Scanning force microscopy (SFM) images were obtained in both the height and phase-contrast mode using a Digital Instruments Dimension 3000 scanning force microscope in the tapping mode. Films for transmission electron microscopy (TEM) were prepared on silicon substrates having a thick layer of silicon oxide. These films were floated onto the surface of a 5 wt % HF solution, transferred to a water bath, and then picked up on a Cu grid. A JEOL 100CX electron microscope operating at 100 kV was used to examine the morphology.

Acknowledgment. This work is based upon work supported by the National Science Foundation under the MRSEC program (UCSB MRL, DMR-0520415 and UMass MRSEC, DMR-0213695), the Army Research Office through its MURI program, and the Department of Energy Office of Basic Energy Science.

JA0608141

(36) Moore, J. S.; Stupp, S. I. *Macromolecules* **1990**, *23*, 65−70.